J. Plasma Fusion Res. SERIES, Vol. 3 (2000) 481–484

Development of Compact Toroid Injector for Large Helical Device and New Concept of Burning Compact Toroid

MIYAZAWA Junichi*, YAMADA Hiroshi, YASUI Kouji, KATO Shinichi, FUKUMOTO Naoyuki[1], NAGATA Masayoshi[1] and UYAMA Tadao[1]

National Institute for Fusion Science, Toki, Gifu 509-5292, Japan

[1]Himeji Institute of Technology, Himeji, Hyogo 671-2201, Japan

(Received: 18 January 2000 / Accepted: 27 May 2000)

Abstract

Compact Toroid Injector named SPICA mk. I (SPheromak Injector using Conical Accelerator) has been developed and successfully assembled on March 1999. Main power source of 40 kJ for CT formation will be installed on March 2000. Simulation result shows that CT kinetic energy of 7 kJ is achievable with this bank in one-stage operation. As CT density is more than a hundred times larger than that of LHD plasmas, fast ions can effectively react with this dense plasmoid. Investigation result on this burning CT concept is also given.

Keywords:

compact toroid, SPICA, point-model simulation, glow discharge, burning CT, advanced fusion

1. Introduction

Compact toroid (CT) injection experiment is intended to fuel dense plasmoid into large and hot plasma of Large Helical Device (LHD). CT is dense plasmoid usually generated as a spheromak, and can be accelerated electro-magnetically to several hundreds of km/s [1]. High-speed CT can penetrate into core region due to the large kinetic energy, which is comparable to the magnetic potential energy at the core region. CT magnetic field decays resistively inside the main plasma and dense plasma confined inside CT is then released. Computed trace of an injected CT inside LHD is three-dimensional reflecting the helical structure [2]. This can be utilized for momentum injection because CT can fuel its contents along with the magnetic field.

A compact toroid injector named SPICA mk. I (SPheromak Injector using Conical Accelerator) has been developed. Conical shape is adopted in the design of inner- and outer-electrode at acceleration part to adiabaticaly compress the CT. Attention has been paid to obtain high acceleration efficiency [3]. SPICA mk. I was successfully assembled on March 1999. Main power source for CT formation, which consists of 20 kV/40 kJ capacitor bank, will be installed on March 2000.

As CT density is more than a few hundreds times larger than that of conventional fusion plasmas, fast ions trapped inside the main plasma can effectively react with this dense plasmoid. If one chose so-called advanced fuels such as ^{3}He, ^{6}Li, and ^{11}B together with hydrogen isotopes, it is possible to provide large fusion energy as the kinetic energy of charged particles, not neutrons. High-energy charged particles generated by this beam-CT fusion can heat the main plasma, and strong core heating has been often related to improved confinement.

In this paper, simulated waveforms of 20 kV/40 kJ capacitor bank applied to SPICA mk. I are given together with some results of the glow discharge

*Corresponding author's e-mail: miyazawa@LHD.nifs.ac.jp

experiment. Investigation results on beam-CT fusion (burning CT) are discussed in the section prior to summary.

2. Simulated Waveforms of SPICA mk. I and Glow Discharge Experiment

A capacitor bank of 20 kV/40 kJ will be installed into SPICA mk. I on this March. This bank is designed for CT formation and another CT acceleration bank should be prepared after the installation of formation bank and initial formation experiments. Although SPICA is equipped with two inner-electrodes isolated from each other, it is possible to connect them electrically and form one-stage plasma gun. This one-stage operation is intended for the initial experiment using formation bank only, and detailed consideration is given in ref. 3. There will be some problems expected in this one-stage operation, such that the blowby phenomena [3], the quality of CT, which might be elongated because of the long acceleration time in one-stage operation, and small acceleration efficiency due to the loss in CT formation process, etc. On the other hand,

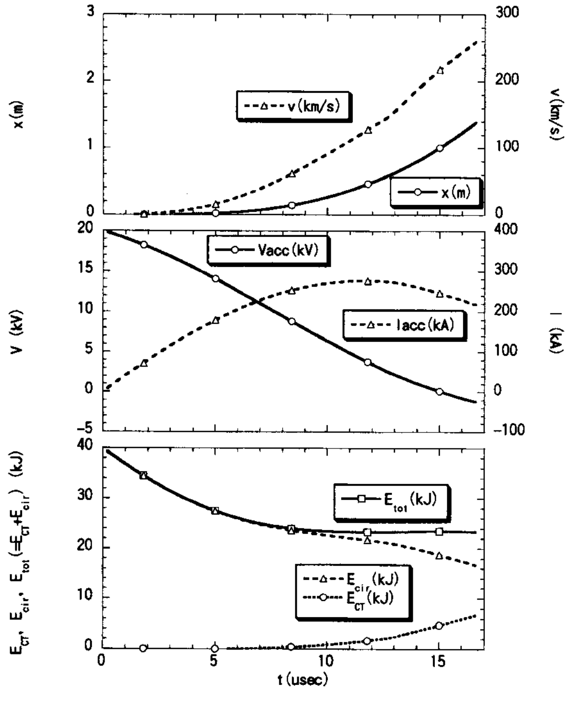

Fig. 1 Simulated waveforms of SPICA mk. I. Point-model [3] is solved using the fourth order Runge-Kutta method. CT mass of 0.2 mg, circuit resistivity of 20 mΩ, and external inductance of 0.48 μH are assumed. As for the electrode geometry, see ref. 3.

one-stage operation has merits in its simple trigger system and reduced cost. Calculated waveforms for one-stage operation in SPICA mk. I are shown in Fig. 1. Efficiency defined as the ratio of CT kinetic energy to bank energy depends on CT mass, circuit resistivity, and external inductance of the circuit. Most of all, CT mass is controllable as it depends on the gas injection rate into the formation part. In this case, the optimum CT mass is 0.2 mg, of which waveforms are drawn in Fig. 1, and 17 % of bank energy is translated into CT kinetic energy (CT kinetic energy of 7 kJ is obtained). This kinetic energy corresponds to the potential energy of 1.4 T magnetic field (when CT volume is 5×10^{-3} m^3).

Glow discharge (GD) cleaning is a powerful wall conditioning technique and adopted in SPICA mk. I. As SPICA is co-axial magnetized plasma gun, one can perform co-axial GD with magnetic field in the axial direction. Stable helium GD is obtained in the pressure p_0 of 15–20 Pa, without bias magnetic field. GD plasma breaks down at voltage of about 1 kV, and in the stable phase, voltage drops to 250–300 V with current of up to 0.5 A (constant current operation). Gap length d between inner- and outer-electrode of formation part is 0.065 m, and therefore p_0d for GD break down is about 1 m·Pa, or 7 mm·torr. After GD breaks down, axial magnetic field is gradually increased. When the magnetic field is increased to about 50 gauss, visible light emission from GD decreases, and localized emission is observed at the plasma periphery (Fig. 2). Localized emission seems unstable, although applied voltage shows no arcing behavior. If one assume He ion temperature of 10 eV, ion Larmor radius is calculated to

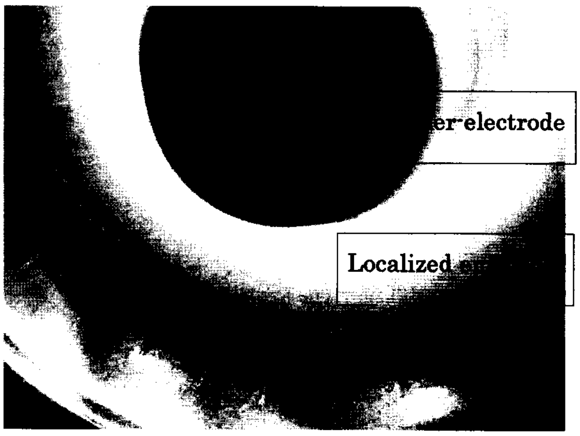

Fig. 2 Localized emission is observed at the periphery of co-axial GD plasma with axial magnetic field of 50 gauss.

be 0.065 m, which equals the gap length d. This means that GD plasma is affected by the magnetic field. More detailed measurement of the localized emission and hydrogen GD experiment are now in preparation.

3. Discussion on Burnable CT Concept

Fusion experiments with less emission of neutrons and radioisotopes are desired especially in LHD, where large amount of super conducting materials are used and well public acceptance is not yet obtained. There exist some reactions suitable for these requirements, i.e.,

$$^{6}\mathrm{Li} + \mathrm{p} \rightarrow {}^{3}\mathrm{He} + \alpha + 4.02\ \mathrm{MeV}\,, \tag{1}$$

$$^{7}\mathrm{Li} + \mathrm{p} \rightarrow 2\alpha + 17.348\ \mathrm{MeV}\,, \tag{2}$$

$$^{11}\mathrm{B} + \mathrm{p} \rightarrow 3\alpha + 8.682\ \mathrm{MeV}\,. \tag{3}$$

These fusion reactions involve neither deuterium nor tritium and emit neither neutrons nor radioisotopes. Fusion reactor scenario that involves reactions above has been investigated from the early stage of fusion study [4]. Such a scenario, however, inevitably needs high temperature, high density, and long energy confinement time. This is because fusion cross-sections of (1)-(3) are small in the temperature range of less than 0.1 MeV as shown in Fig. 3 [5]. Although it seems difficult to use these advanced fusion reactions for reactor design, it is still meaningful to carry out fusion experiments with less neutron emission. This is because there are many unsolved problems related to burning plasmas, i.e., α particle confinement and its heating efficiency, instabilities like TAE, radial electric field due to the orbit loss of α particles, and accumulation of cold He ash, etc. LHD is equipped with two 180 keV neutral beam injection systems (NBI) and ion cyclotron heating systems (ICH). These heating devices can afford high-energy particles. Therefore, if the density of target particle like boron is large enough, fusion reactions will occur in measurable scale.

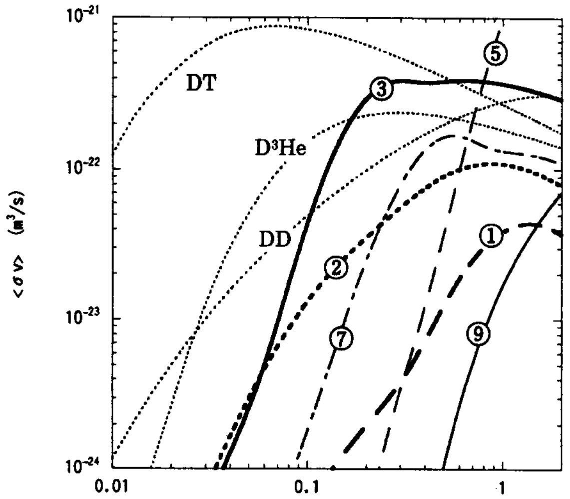

Fig. 3 Fusion cross-section as a function of ion temperature T_i. Number indicates reaction type and identical to the equation number in the article. Cross-sections of eqs. (4), (6) and (8) are small (< 10^{-25} m^3/s at T_i < 2 MeV) and not illustrated.

Note that even advanced fuels cannot be free from the neutron and radioisotope emission. There are some unfavorable side-reactions as below;

$$^{6}\mathrm{Li} + \mathrm{p} \rightarrow \gamma + {}^{7}\mathrm{Be} + 5.606\ \mathrm{MeV}\,, \tag{4}$$

$$^{7}\mathrm{Li} + \mathrm{p} \rightarrow \mathrm{n} + {}^{7}\mathrm{Be} - 1.644\ \mathrm{MeV}\,, \tag{5}$$

$$^{10}\mathrm{B} + \mathrm{p} \rightarrow \gamma + {}^{11}\mathrm{C} + 8.691\ \mathrm{MeV}\,, \tag{6}$$

$$^{10}\mathrm{B} + \mathrm{p} \rightarrow \alpha + {}^{7}\mathrm{Be} + 1.146\ \mathrm{MeV}\,, \tag{7}$$

$$^{11}\mathrm{B} + \mathrm{p} \rightarrow \gamma + {}^{12}\mathrm{C} + 15.957\ \mathrm{MeV}\,, \tag{8}$$

$$^{11}\mathrm{B} + \mathrm{p} \rightarrow \mathrm{n} + {}^{11}\mathrm{C} - 2.765\ \mathrm{MeV}\,. \tag{9}$$

Cross-sections of above reactions are small compared with reactions (1)-(3) (see Fig. 3). Only endothermic reactions emit neutrons (see eqs. (5) and (9)) and radioisotopes produced by these reactions are less harmful as they have short half-life (^{7}Be: 53.3 days, ^{11}C: 20.39 min.).

It seems better to chose boron for burning CT investigation because the maximum cross-section of reaction (3) is larger than that of others, and neutrons are emitted only in high temperature range. To use boron, of which the boiling point is extremely high (3931 K), as a working gas to form CT, there are at least two ways. One is to use the vapor of decaborane ($B_{10}H_{14}$), of which the boiling point is 486 K, and the other is to use the diborane gas (B_2H_6). The better is the decaborane vapor because the ratio of boron ion density to electron density (0.156) is larger than that of the diborane gas (0.125) when they are fully ionized. Note that the ratio in case of pure boron is 0.2.

Before going into details of beam-CT fusion investigation, we should note that $<\sigma v>$ shown in Fig. 3 are obtained by averaging σv with the Maxwellian distribution while assuming the same temperature of both particles in each reactions. In our case, high-energy component generated by NBI and/or ICH should have much higher effective temperature T_1 than that of the target (CT) plasma T_0. When applying Fig. 3 in this case, we should use reduced temperature T_r defined as below;

$$T_r = \frac{m_r}{m_0} T_0 + \frac{m_r}{m_1} T_1\,, \tag{10}$$

where m_0 is mass of target particle, m_1 is mass of high-energy particle, and m_r is reduced mass ($m_r = m_0 m_1/(m_0 + m_1)$). In the case of p – ^{11}B reaction $T_r = (11/12)\ T_1$ in the limit of $T_0 = 0$, for instance.

To estimate the order of fusion energy density released from beam-CT fusion, we assume boron density $n_B = 10^{22}$ m^{-3}, and density of high-energy protons $n_p^* = 10^{16}/T_1$ m^{-3} (T_1 in MeV). This assumption makes it possible to determine the optimum T_1 in constant pressure of the high-energy component. This model also approximate steady-state LHD plasma heated by 7.5 MW/150 keV NBI, where n_p^* is estimated to be of order 10^{17} m^{-3} with the slowing down time of 0.01 sec. Production rate of α particles per unit volume as a function of T_1 is calculated for p-B reactions and shown in Fig. 4, together with that of ^{7}Be and neutrons. Natural boron, which contains 80 % of ^{11}B and 20 % of ^{10}B, is assumed to contained in the target CT. Note that if one separates ^{11}B from natural boron, the radioisotope emission can be largely decreased. As can be seen in the figure, 3×10^{17} m^{-3}s^{-1} of α production rate is obtained at T_1 = 200 keV. Higher T_1 is not necessarily effective to increase α production rate in this model. Averaged α particle energy is given as 2.46 MeV (from eqs. (3) and (7)), and therefore the fusion energy density released as the kinetic energy of α particles is as large as 0.118 MW/m^3. This is the same order as NBI heating power density. In LHD, deuterium-deuterium (DD) experiment is supposed to produce neutrons at a rate of 2.4×10^{16} neutrons/sec, or considering LHD plasma volume of ~26 m^3, 9.2×10^{14} neutrons/(m^{3}s) in average. Same neutron production rate is only obtained in the high temperature range of $T_1 > 1$ MeV in p-B reaction. Moreover, as the CT volume of about 5×10^{-3} m^3 in our case is very small compared with the LHD volume, total neutron emission rate of burning CT is five thousands times smaller than that of DD experiment. Fusion energy density released from DD plasma as kinetic energy of charged particles is about 720 W/m^3 and more than a hundred times smaller than that of burning CT, on the other hand.

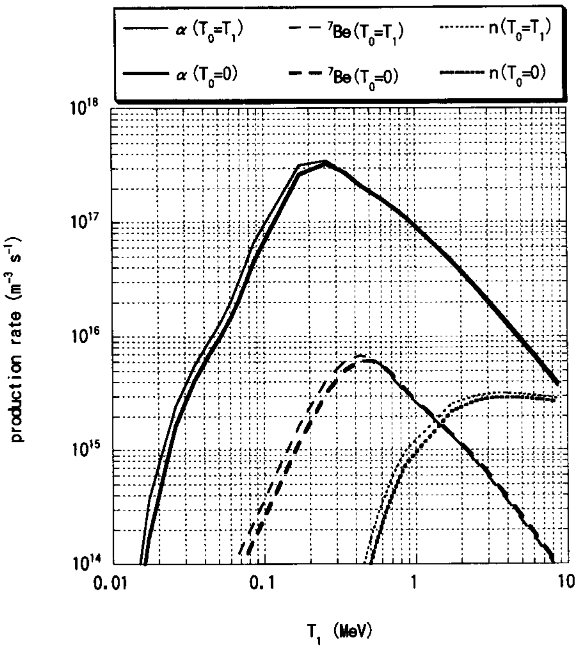

Fig. 4 Production rates of α particle, ^{7}Be, and neutron, from p-B reactions. For each particles, two extreme cases of $T_0 = T_1$ and $T_0 = 0$ are shown.

4. Summary

Discharge simulation result of SPICA mk. I energized by 20 kV/40 kJ capacitor bank shows that CT kinetic energy of 7 kJ can be obtained. This bank will be installed on this March. Initial test of helium glow discharge has been carried out and localized emission is observed when 50 gauss of magnetic field is applied. As a new scenario for confinement improvement by CT injection, other than density peaking induced by center fueling or momentum injection effect, the burning CT concept was examined. Fusion energy density released as kinetic energy of charged particles from the burning CT is more than a hundred times larger than DD experiment in LHD, and the order is the same as NBI heating. Meanwhile, neutron emission is negligibly small compared with DD experiments. Fusion related experiment with less neutron emission is possible using this burning CT in LHD.

References

[1] For example, J.H. Hammer *et al.*, Phys. Rev. Lett. **61**, (1988) 2843.

[2] J. Miyazawa *et al.*, Jpn. J. Appl. Phys. **37** (1998) 6620.

[3] J. Miyazawa *et al.*, NIFS-614 (NIFS Research Report, 1999); J. Miyazawa *et al.*, Fusion Eng. and Design, to appear.

[4] For example, W.M. Nevins, J. Fusion Energy **17** (1998) 25; also, D.C. Moreau, Nucl. Fusion **17** (1977) 13

[5] W.A. Fowler *et al.*, Ann. Rev. Astron. Astrophys. **13** (1975) 69; see also, J. McNally, Jr. *et al.*, ORNL/TM-6914.